Moiré Reduction Method for Visually Equivalent Light Field Display Using Special Barrier Aperture Structure

Munekazu Date[1], Tokinobu Mitasaki[1], Ayumi Matsumoto[1], Masaki Kitahara[1]

munekazu.date.zf@hco.ntt.co.jp
[1]NTT Computer and Data Science Laboratories, Nippon Telegraph and Telephone Corporation
Keywords: light field display, moiré, parallax barrier

ABSTRACT

A visually equivalent light field 3D (VELF3D) display is a parallax-barrier-type autostereoscopic 3D display. Since stripes of the barrier and pixels are in parallel, moiré occurred, when the barrier is placed on the screen. In this paper, we suppressed moiré by only providing unevenness in the aperture shape of the barrier.

1 Introduction

In multi-view displays or light-field displays, different images can be seen depending on the viewing direction. Improving the directional density will not only allow smooth motion parralax for large motion of head position, but also to respond to minute changes in the pupil position. Furthermore, accommodation can also be satisfied if the directional density is improved so that different rays enter the pupil at the same time. However, conventional displays have a trade-off in that increasing the directivity number reduces the resolution.

Therefore, by presenting an image at an intermediate viewpoint position that is optically mixed (linear blending) of images from adjacent viewpoints in a multi-view display, it is possible to show a linearly interpolated image that matches the viewpoint position, resulting in a smooth and accurate motion parallax could be presented.

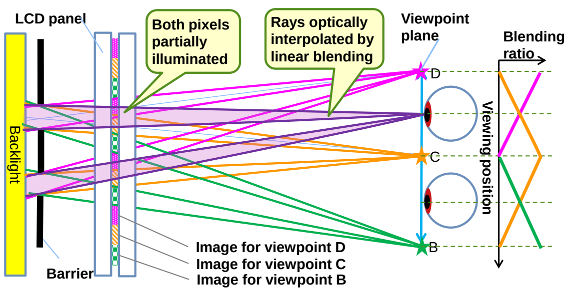

Fig.1 Visually equivalent light field 3D display.

At first, we performed projection type display using a special shape aperture [1], but the image distortion was too large. Therefore, as shown in Fig. 1, we proposed to match the pixel pitch and the width of the barrier aperture in a parallax barrier-type autostereoscopic 3D display. The range of pixels illuminated by the backlight is proportional to the amount of movement of the pupil position. As can be seen from the graph in the figure, the luminance of the each viewpoint image changes linearly with the observation position, so linear blending is performed at intermediate viewpoints [2]. In other words, rays of light field are interpolated. So, we call it a visually equivalent light field 3D (VELF3D) display because it is perceived as equivalent to real light rays for human vision even at intermediate viewpoints.

Since the barrier was placed between the liquid crystal panel and the backlight in the originally manufactured display, the barrier stripe was observed through the liquid crystal display (LCD) panel. Since the light is diffused by the comb electrode in the panel, the image of the barrier is effectively blurred, so moiré was not produced. However, in the case of modifying a commercially available tablet [3], it was difficult to modify the tablet body and add a parallax barrier inside. Therefore, we decided to put a barrier on the surface of the touch panel of the tablet, but it caused moiré.

When installing a barrier on the top surface of the touch panel, the barrier must be a thin film so as not to interfere with the operation of the touch panel. Therefore, it is not realistic to add other components to prevent moiré. In this paper, we report that moiré can be suppressed by simply changing the aperture shape of the barrier printed on the film.

2 Moiré Reduction

In a visually equivalent light field display, the moiré fringes generated by the interference of the baseband, constitute the viewpoints of the multi-view display, and interpolate viewpoints by linear blending [4]. Therefore, it is considered that the moiré in this study is caused by the interference of high-frequency components. Therefore, we decided to suppress the high spatial frequency components of the barrier aperture. The transmittance of the parallax barrier for horizontal coordinate x is given by

$$Comb_{p_b}(x) * Rect_{p_b\alpha_b}(x),$$

where * is the convolution, p_b and α_b are the barrier pitch and its aperture ratio respectively. The rectangular function Rect and the comb function Comb are

$$Rect_a(x) = \begin{cases} 1 & |x| \le \frac{a}{2}, \\ 0 & others \end{cases}$$

$$Comb_a(x) = \sum_{i=-\infty}^{\infty} \delta(x - ai),$$

where δ is the Dirac delta function. Considering this transmittance in spatial frequency space is

$$\frac{1}{p_b} Comb_{1/p_b}(f) \frac{\sin \pi f p_b \alpha_b}{\pi f}.$$

It is a comb function with envelope of a sinc function ($\mathrm{sinc}\,\theta = \sin\theta / \theta$). Since the sinc function has a long tail, there are high frequency components. Therefore, we applied Gaussian low-pass filter that rapidly decays both in real space and frequency space. The Gaussian function in real space is

$$Gauss_a(x) = \frac{a}{\sqrt{2\pi}} e^{-\frac{x^2}{2a^2}}.$$

The transmittance of proposed barrier is expressed as

$$Comb_{p_b}(x) * Rect_{p_b \alpha_b}(x) * Gauss_{\sigma p_b \alpha_b}(x).$$

σ is a barrier design parameter. This function is in frequency space

$$\frac{1}{p_b} Comb_{1/p_b}(f) \frac{\sin \pi f p_b \alpha_b}{\pi f} \frac{\sigma p_b \alpha_b}{\sqrt{2\pi}} e^{-\frac{(\sigma p_b \alpha_b)^2 f^2}{2}}$$

Therefore, it can be seen that the high-frequency component decays rapidly due to the exponential term.

Transmittance of a single slit of the barrier can be expressed as following, a difference of two error functions,

$$\begin{aligned} &Rect_{p_b \alpha_b}(x) * Gauss_{\sigma p_b \alpha_b}(x) \\ &= \frac{1}{2}\left\{ \mathrm{erf}\left(\frac{x + p_b \alpha_b / 2}{\sqrt{2}\sigma p_b \alpha_b}\right) - \mathrm{erf}\left(\frac{x - p_b \alpha_b / 2}{\sqrt{2}\sigma p_b \alpha_b}\right)\right\}. \end{aligned}$$

3 Experiment and Results

It is very difficult to manufacture a barrier with gray scale transmittance at the periphery of the aperture width of several tens of micrometers. Therefore, we considered realizing it with binary transmittance. As with the area gradation, the transmittance averaged in the direction parallel to the barrier is set to the desired value. In addition, we decided to make the periphery of the aperture uneven because the requirement for resolution in printing would be severe if halftone dots were used. As shown in Fig. 2, by setting the aperture between the error functions that are slightly shifted to the left and right, the average transmittance becomes the difference between the error functions.

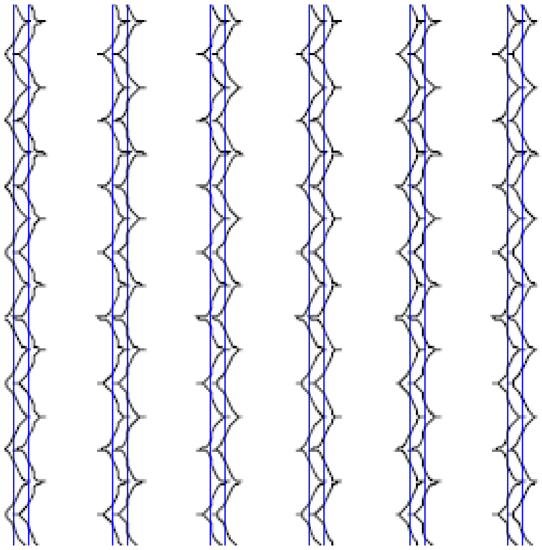

Fig.2 Barrier aperture shape (σ=0.375). The blue line indicates the conventional straight aperture.

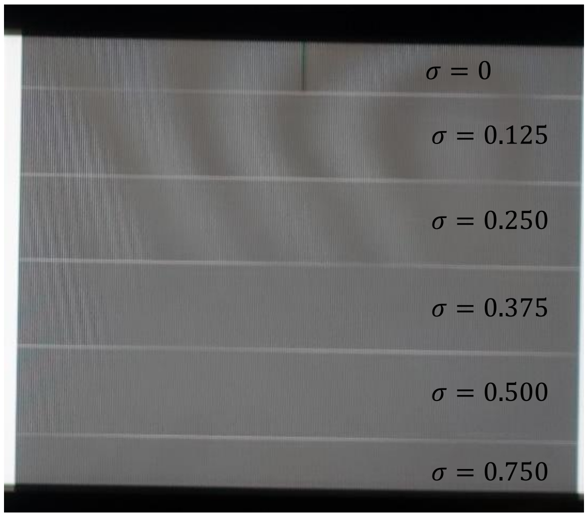

Fig. 3 Change of moiré with parameter σ.

As the parameter σ increases, the unevenness of the barrier increases, and the suppression of high-frequency components also increases. However, in principle, the condition for linear blending is σ=0, so it is necessary to construct a display with the minimum σ that can suppress moiré. Therefore, we fabricated barriers with different values of σ and evaluated the occurrence of moiré. White full screen image is displayed on the screen of iPad Pro 11 inch. The barrier film is placed on the touch panel, and set the angle at which the moiré is the roughest. Therefore, the RGB stripe of the screen and the barrier stripe should be parallel.

The results are shown in Figure 3. About five thick moiré lines in the photograph are the moiré lines that we want to suppress. The fine moiré is the moiré with the pixels of the camera used for shooting. As can be seen from the photograph, it can be suppressed when σ is smaller than 0.375. Also, moiré suppression is not continuous, but seems to change with a threshold.

By attaching a film with σ = 0.375 to the surface of an 11-inch tablet iPad Pro, we fabricated a display device without moiré as shown in Fig. 4 [4]. In order to display seven viewpoints, the barrier period p_b = 223.58 µm is slightly smaller than 7 times the sub-pixel width of 32 µm, so that the rays are focused at a viewing distance of about 45 cm. The aperture width is 1/7 of the barrier period. As can be seen from the photographs, no moiré occurred and good 3D images could be observed.

Fig. 4 Prototype of tablet-type VELF3D display using our proposed barrier.

4 Discussions

Moiré was suppressed by the pattern of the proposed barrier. However, it is unclear what the condition of σ=0.375 means. Therefore, we considered common spatial frequency component of the barrier aperture and the panel pixel causes moiré, and focused on the lowest common frequency.

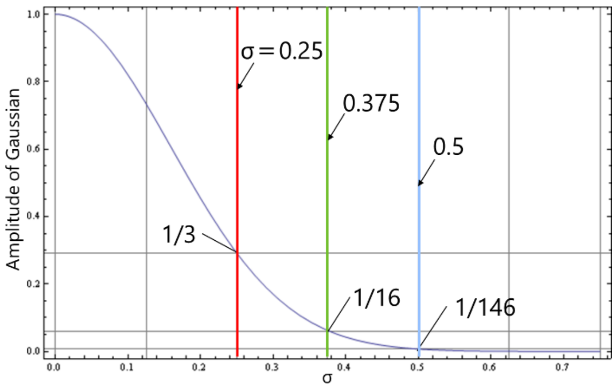

Fig. 5 The amplitude of gaussian at the moiré frequency depending on σ.

The amplitude of Gaussian at the lowest spatial frequencies is shown in Fig. 5. It should be in proportion to amplitude of moiré. As σ increases, it approaches to zero, indicating that moiré is suppressed. The amplitude is about 1/3 of σ=0 when σ=0.25 and about 1/16 when σ=0.375. As you can see from Fig. 2, moiré is significantly different and amplitude of Gaussian cannot explain the phenomena enough.

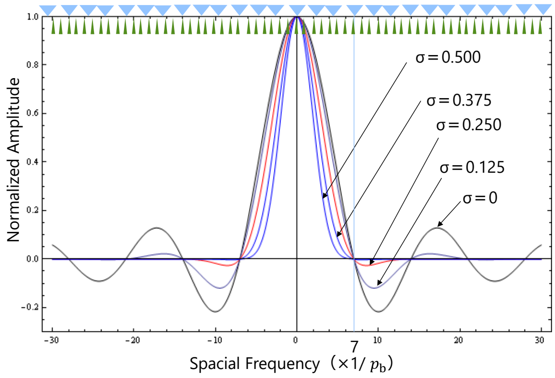

(a)

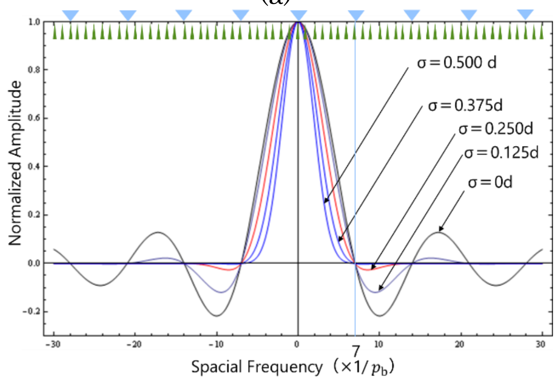

(b)

Fig. 6 Variation of envelope function of spatial frequency characteristics with σ. ▲ is the barrier period, and ▼ is the spatial frequency corresponding to the pixel period. pb is the barrier pitch. (a)RGB vertical stripe panel 7 viewpoint configuration, (b) RGB horizontal stripe panel 7 viewpoint configuration.

Fig. 6(a) shows plots of the envelope of the frequency characteristics by changing the barrier parameter σ. The horizontal axis is the spatial frequency normalized by the period of the barrier aperture, and the vertical axis is the amplitude normalized by the value at spatial frequency 0. These are the calculation results for a multi-view display configuration with 7 viewpoints on an RGB vertical stripe panel. Since peaks of frequency matches at the position of spatial frequency 7, it is assumed that moiré occurs at this frequency.

The curve in the graph is the multiplication of the sinc function and Gaussian, corresponding to the envelope of comb shaped spectrum. All curves intersect the horizontal axis at a spatial frequency of 7, and the amplitude at the frequency becomes zero. When σ≤0.25, the envelope is not 0 in the region where the spatial frequency is greater than 7, and the spatial frequency above 7 is not sufficiently suppressed. However, when σ ≥ 0.375, the value of the envelope becomes almost zero from a spatial frequency slightly smaller than 7. That is, it was found that it was necessary to suppress the periphery of the frequency in order to eliminate the moiré.

As shown in Fig. 6(b), frequency peaks of barrier is different for 7 viewpoint display with horizontal RGB stripe screen. Since this condition does not depend on the number of viewpoints of the display, it is considered to be a universal condition for moiré suppression.

5 Conclusions

Usually, moiré caused by interference between parallax barriers or lenticular lenses and display pixels was eliminated by oblique placement. In this paper, we proposed a new method to solve this problem by changing the shape of the barrier aperture, and demonstrated that it was sufficiently effective in suppressing moiré.

With this method, it is possible to construct a VELF3D display that uses the parallax barrier and pixel stripes in a parallel arrangement, even though the barrier can be placed on the screen. And we developed portable VELF3D display without breaking the tablet computer.

References

[1] T. Kawakami, M. Date, M. Sasai, and H. Takada: “Optical Linear Blending of Viewing Zones Using Convolution of Iris for Smooth Motion Parallax Autostereoscopic 3D Display,” Journal of Display Technology, 12(2), pp. 143–152, 2016.

[2] M. Date, Y. Tanaka, M. Isogai, S. Shimizu, and H. Kimata: “Table Top Visually Equivalent Light Field 3D Display Using 15.6-inch 4K LCD Panel,” SID Display Week 2019, 56-5, pp. 791–794, 2019.

[3] M. Date, S. Shimizu, S. Yamamoto: “Visually Equivalent Light Field 3D for Portable Displays,” IEEE Transactions on Industry Applications, 58(5), pp. 5659–5666, 2022.

[4] M. Date, S. Shimizu, H. Kimata, D. Mikami, and Y. Kusachi, “Depth Range Control in Visually Equivalent Light Field 3D,” IEICE Transactions on Electronics, E104.C, pp. 52–58, 2021.